# Numerical Study of Thermal Conduction Influence on Homogeneity of InGaAs Crystals

By

Satoshi ADACHI[1], Yasuyuki OGATA[1], Izumi YOSHIZAKI[1], Satoshi MATSUMOTO[1], Naokiyo KOSHIKAWA[1], Masahiro TAKAYANAGI[1], Kyoichi KINOSHITA[1] and Shin-ichi YODA[1]

**Abstract** : In order to investigate suitable ampoule configuration for crystal growth experiments under microgravity for obtaining homogeneous crystals, theoretical modeling and numerical simulation are carried out. From the model, a new index named the two-dimensionality is introduced. By calculating the two-dimensionality in a case of a sample diameter of 20 mm, it is found that a combination of an InGaAs seed crystal and a BN crucible is inappropriate from the viewpoint of homogeneity. To find a more appropriate combination of a seed and a crucible materials, a dominant mechanism of two-dimensionality deterioration is discussed. By considering the dominant mechanism, it is successfully obtained of the more suitable combination.

**Key words** : Microgravity experiment, Traveling liquidus-zone method, Theoretical modeling, Numerical simulation, Homogeneous crystal

## 1. Introduction

InGaAs bulk crystals have been expected to be the next generation materials, which are used for wafers for optoelectronic devices. However, it is difficult to grow homogeneous InGaAs crystals on earth. One of the reasons for inhomogeneity occurrence is mass transport by thermal convection. To suppress thermal convection sufficiently so that the mass transport can be dominated by diffusion process, use of microgravity condition is one of the most effective ways. Therefore, we have planned to carry out a crystal growth experiment under microgravity to grow a homogeneous crystal. We have already developed a new crystal growth technique for the homogeneous crystal growth under microgravity, named the traveling liquidus-zone (TLZ) method [1, 2]. The TLZ method has a feature that a one-dimensional model of the TLZ method precisely predicts the growth rate [3]. By translating a sample with the predicted rate, temperature at the growth interface is kept constant. Thus homogeneous crystals are grown. The TLZ method works fine even on the ground if a sample diameter is small enough to reduce the convection influence on the mass transport, for example, 2 mm in diameter. Homogeneous InGaAs and SiGe crystals with 2 mm in diameter have been successfully obtained on the ground. Unfortunately, in larger sample diameter cases such as 5 mm or more in diameter, the homogeneity deteriorates due to increase of the convection influence on the ground. To quantitatively indicate the convection influence, we have already established a quantitative expression named the convection influence index $\chi$ [4]. By calculating the radially averaged index $\bar{\chi}$ in various sample diameters, it was found that the maximum sample diameter may be 2 mm to grow homogeneous crystals on the ground. However, since the convection is suppressed under microgravity, homogeneous

[1] Institute of Space and Astronautical Science, Japan Aerospace Exploration Agency

samples with more than 2 mm in diameter may be grown. Therefore, we have investigated the maximum sample diameter so that homogeneous crystals can be grown under microgravity by using numerical simulation. From the simulation results under the microgravity condition of $10^{-5}g$, it was found that the $\bar{\chi}$ reduction is insufficient in cases of more than 10 mm in diameter. In addition, the $\bar{\chi}$ in a region of more than 10 mm is almost constant. The homogeneity is also not excellent in this region. This suggests that another mechanism affecting the $\bar{\chi}$ exists Thus the mechanism is investigated in this study. First, gravity dependency of the $\bar{\chi}$ is obtained whether the microgravity level of $10^{-5}g$ is enough to suppress the convection. Second, we introduce a new index named the two-dimensionality by expanding the one-dimensional TLZ model to a two-dimensional one in order to investigate the mechanism. Then we calculate this index by using results from numerical simulation and discuss a method of reducing the two-dimensionality.

## 2. Convection Influence

The popular index representing mass transport affected by convection is the Sherwood number *Sh*. The Sherwood number is defined as

$$Sh = \frac{hL}{D}, \tag{1}$$

where $h$ is the mass transfer coefficient, $L$ the characteristic length, $D$ the diffusion coefficient. By using the mass transfer coefficient, a one-dimensional mass transport equation in a steady state is written as

$$-D\frac{\partial C}{\partial z} + C v = h\Delta C, \tag{2}$$

where $C$ and $v$ are concentration and flow velocity, respectively. If there is no convection, that is, $v$ =0, the Sherwood number is rewritten as

$$Sh = \frac{-D\dfrac{\partial C}{\partial z}L}{\dfrac{\Delta C}{D}} = -\frac{\partial C}{\partial z} \Big/ \frac{\Delta C}{L}. \tag{3}$$

By calculating Eq. (3), the local Sherwood number at a certain radius can be obtained. This equation is rewritten in the one-dimensional case as

$$Sh = -\frac{\partial C}{\partial z}\Big|_{conv} \Big/ -\frac{\partial C}{\partial z}\Big|_{diff}, \tag{4}$$

where the numerator represents the concentration gradient affected by the convection and the denominator the gradient by only the diffusion. Here, the convection effect is assumed to be written as A. Then the numerator of Eq. (4) is written as

$$-D\frac{\partial C}{\partial z}\Big|_{conv} = -D\frac{\partial C}{\partial z}\Big|_{diff} + A. \tag{5}$$

By substituting Eq. (5) to Eq. (4), the Sherwood number is represented as

$$Sh = 1 + \frac{A}{-D\left.\frac{\partial C}{\partial z}\right|_{diff}}. \tag{6}$$

By considering the representation of Eq. (6), we define a new index a, which is always more than 1, to indicate not only axial mass transport but also radial one. The new index is named the convection influence index $\chi$ [4]. The $\chi$ is expressed as

$$\chi = 1 + \left| \frac{A}{-D\left.\frac{\partial C}{\partial z}\right|_{diff}} \right|. \tag{7}$$

By substituting Eq. (5) to Eq. (7), the $\chi$ is obtained by using the Sherwood number as

$$\chi = 1 + \left| -1 + Sh \right| = \begin{cases} 2 - Sh & (Sh < 1) \\ Sh & (Sh \geq 1) \end{cases}. \tag{8}$$

By radially averaging the $\chi$, the averaged convection influence index $\bar{\chi}$ can be obtained. By using results from numerical simulation, which is described later in detail, the $\bar{\chi}$ is calculated. The $\bar{\chi}$ dependency on sample diameter is shown in Fig. 1. In Fig. 1, closed and open circles represent the calculation results in InGaAs crystal growth under $10^{-5}g$ and in $1\,g$ conditions, respectively. In the 2 mm case, the $\bar{\chi}$ difference between the $10^{-5}g$ and $1\,g$ conditions are negligibly small. This indicates that the 2 mm diameter sufficiently suppresses the convection by the wall effect. The $\bar{\chi}$ under the $10^{-5}g$ condition is also small in the region of more than 2 mm as compared with that under the 1 g condition. However, the $\bar{\chi}$ is around 1.1 and may not be sufficiently small. To understand whether the $10^{-5}g$ condition is enough gravity level to suppress the convection, numerical simulation under various gravity conditions are carried out. The $\bar{\chi}$ dependency on the gravity is shown in Fig. 2. Closed circles represent the calculated $\bar{\chi}$. The horizontal dashed line represents asymptotic line under zero gravity. The dashed line passing the closed circles indicates that the $\bar{\chi}$ is almost the same as the asymptotic value of the $\bar{\chi}$. Therefore, it is found that the gravity of $10^{-5}g$ is enough to suppress the convection sufficiently. On the other hand, the asymptotic value suggests another problem exists, that is, the residual $\bar{\chi}$ value of about 1.1 is not caused by the convection. The reason should be understood to obtain homogeneous crystals.

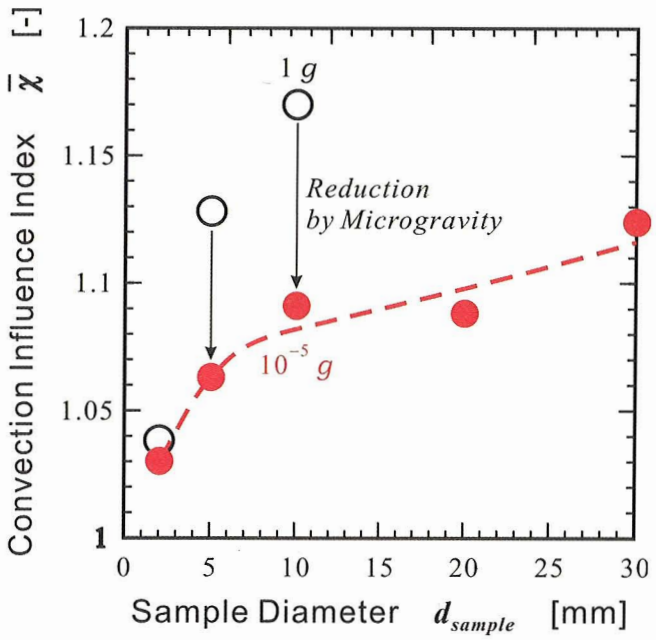


**Fig. 1** $\bar{\chi}$ dependency on sample diameter

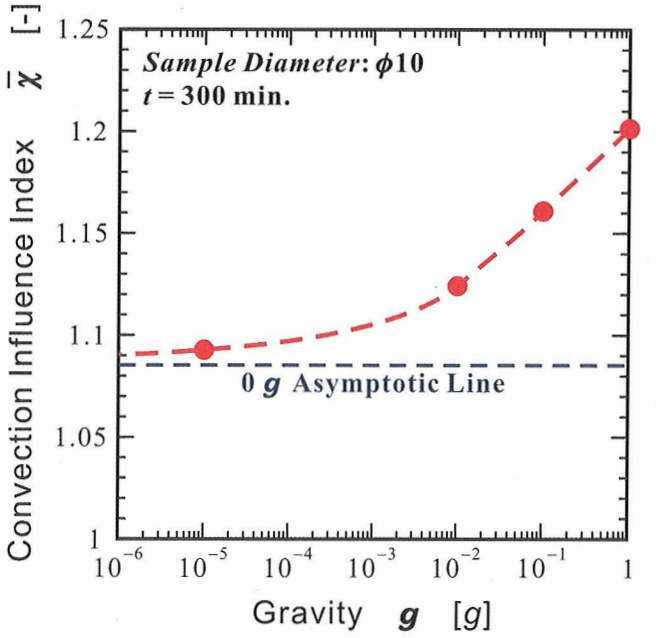


**Fig. 2** $\bar{\chi}$ dependency on gravity

## 3. Two-dimensionality

### 3.1 Theoretical Model

To understand the reason why the $\bar{\chi}$ is not equal to 1 even though the gravity is zero, radial dependency of the local $\chi$ in zero gravity, which expresses radial and axial mass transport at any radius, is obtained first. The dependency is shown in Fig. 3. This figure shows that the $\chi$ is about 1.1 around the axis, while that is more than 1.3 near a crucible wall. Nonuniform $\chi$ profile means inhomogeneous crystal may be grown since a growth rate varies radially. In order to

investigate radial variation of the growth rate, a new model of the TLZ method is required. In this study, the one-dimensional TLZ model is expanded to a two-dimensional one. The one-dimensional model [3] is described as

$$R = -\frac{D}{(C_L - C_S)} \frac{\partial C_L}{\partial T} \frac{\partial T}{\partial z}\bigg|_L . \tag{9}$$

This equation is expanded to a general expression, that is,

$$(C_L - C_S)\boldsymbol{R} \cdot \hat{\boldsymbol{n}} = -D \nabla C_L \cdot \hat{\boldsymbol{n}} , \tag{10}$$

where $\boldsymbol{R}$, $\hat{\boldsymbol{n}}$ are a growth rate vector and a normal unit vector to an interface, respectively. $C_L$ and $C_S$ are concentration in liquid and in solid, respectively. Here, we consider two-dimensional cylindrical coordinates. Thus, an axial coordinate of an interface, $z$, can be expressed as a function of a radial coordinate and time, $r$ and $t$, that is,

$$z = f(r, t) . \tag{11}$$

By using Eq. (11), the normal unit vector is expressed as

$$\hat{\boldsymbol{n}} = \frac{1}{\sqrt{1 + \left(\frac{\partial f}{\partial r}\right)^2}} \left( -\frac{\partial f}{\partial r}, 1 \right) . \tag{12}$$

In addition, $\boldsymbol{R}$ is expressed as

$$\boldsymbol{R} = \left( \frac{\partial r}{\partial t}, \frac{\partial z}{\partial t} \right) = \left( \frac{\partial r}{\partial t}, \frac{\partial f}{\partial t} + \frac{\partial f}{\partial r} \frac{\partial r}{\partial t} \right) . \tag{13}$$

By substituting Eqs. (12) and (13) to Eq. (10), Eq. (10) is rewritten as

$$(C_L - C_S) \frac{\partial f}{\partial t} = -D \left( \frac{\partial C_L}{\partial z} - \frac{\partial C_L}{\partial r} \frac{\partial f}{\partial r} \right) . \tag{14}$$

The same assumption of the one-dimensional TLZ model is introduced, that is,

$$\frac{\partial C_L}{\partial z}\bigg|_{z=int} = \frac{\partial C_L}{\partial T}\bigg|_{z=int} \frac{\partial T}{\partial z}\bigg|_{z=int} , \text{ and} \tag{15}$$

$$\frac{\partial C_L}{\partial r}\bigg|_{z=int} = \frac{\partial C_L}{\partial T}\bigg|_{z=int} \frac{\partial T}{\partial r}\bigg|_{z=int} . \tag{16}$$

Equations (15) and (16) are substituted to Eq. (14). Thus a two-dimensional TLZ model of

$$(C_L - C_S) \frac{\partial f}{\partial t} = -D \frac{\partial C_L}{\partial T} \left( \frac{\partial T}{\partial z} - \frac{\partial T}{\partial r} \frac{\partial f}{\partial r} \right)_L \tag{17}$$

is obtained. By comparing Eq. (17) with Eq. (9), the one-dimensional model, it is found that Eq. (17) is exactly the same as Eq. (9) if the second term inside the parenthesis of the right side of Eq. (17) is zero. Therefore, the second term represents a factor changing a growth rate. We define a new index as a ratio of the second term to the first term, that is,

$$\delta = \left. -\frac{\partial T}{\partial r}\frac{\partial f}{\partial r} \right/ \frac{\partial T}{\partial z} \tag{18}$$

and name this index the two-dimensionality. If the two-dimensionality is not zero, the growth rate will change. Therefore, the condition of $\delta = 0$ is a ideal condition from the viewpoint of the homogeneous crystal growth.

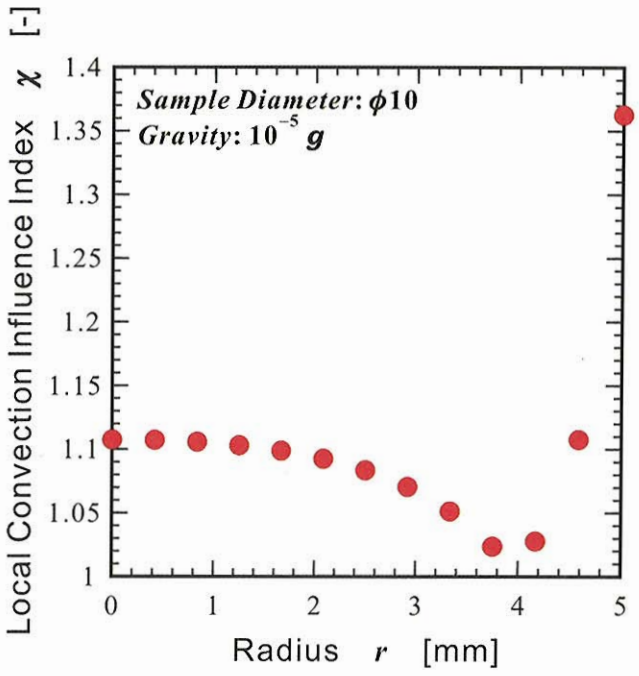


**Fig. 3** Radial dependency of local χ

### 3.2 Governing Equations

In order to calculate Eq. (18), temperature gradients along $r$- and $z$-directions and an interface shape are required. To obtain these parameters, two-dimensional numerical simulations are carried out. In the simulation, the energy transport equation, the mass transport equation, the stream function equation, the vorticity transport equation, the energy balance equation and the mass balance equation are simultaneously solved. We use the boundary fitted coordinate (BFC) method [5-11], which is a kind of finite difference method, in order to solve these equations. The BFC method solves the governing equations that are transformed from the physical space to the computational space. The transformed governing equations are expressed as Eqs. (19)-(25), that is,

$$\begin{aligned} &\rho C_p\left\{\frac{\partial T}{\partial t} - \frac{1}{J}\left(z_\eta T_\xi - z_\xi T_\eta\right)\frac{\partial r}{\partial t} - \frac{1}{J}\left(-r_\eta T_\xi + r_\xi T_\eta\right)\frac{\partial z}{\partial t}\right\} - \rho C_p \frac{1}{r}\frac{1}{J}\left(\psi_\xi T_\eta - \psi_\eta T_\xi\right) \\ &= \kappa\frac{1}{J^2}\left(\alpha T_{\xi\xi} - 2\beta T_{\xi\eta} + \gamma T_{\eta\eta}\right) + \kappa\frac{1}{r}\frac{1}{J}\left(z_\eta T_\xi - z_\xi T_\eta\right) \end{aligned}, \tag{19}$$

$$\frac{\partial C_L}{\partial t}-\frac{1}{J}\left(z_\eta C_{L\xi}-z_\xi C_{L\eta}\right)\frac{\partial r}{\partial t}-\frac{1}{J}\left(-r_\eta C_{L\xi}+r_\xi C_{L\eta}\right)\frac{\partial z}{\partial t}-\frac{1}{r}\frac{1}{J}\left(\psi_\xi C_{L\eta}-\psi_\eta C_{L\xi}\right)$$
$$=D_L\frac{1}{J^2}\left(\alpha C_{L\xi\xi}-2\beta C_{L\xi\eta}+\gamma C_{L\eta\eta}\right)+D_L\frac{1}{r}\frac{1}{J}\left(z_\eta C_{L\xi}-z_\xi C_{L\eta}\right), \tag{20}$$

$$\frac{\partial C_S}{\partial t}-\frac{1}{J}\left(z_\eta C_{S\xi}-z_\xi C_{S\eta}\right)\frac{\partial r}{\partial t}-\frac{1}{J}\left(-r_\eta C_{S\xi}+r_\xi C_{S\eta}\right)\frac{\partial z}{\partial t}$$
$$=D_S\frac{1}{J^2}\left(\alpha C_{S\xi\xi}-2\beta C_{S\xi\eta}+\gamma C_{S\eta\eta}\right)+D_S\frac{1}{r}\frac{1}{J}\left(z_\eta C_{S\xi}-z_\xi C_{S\eta}\right), \tag{21}$$

$$-rJ^2\omega=\alpha\psi_{\xi\xi}-2\beta\psi_{\xi\eta}+\gamma\psi_{\eta\eta}-\frac{J}{r}\left(z_\eta\psi_\xi-z_\xi\psi_\eta\right), \tag{22}$$

$$\frac{\partial\omega}{\partial t}-\frac{1}{J}\left(z_\eta\omega_\xi-z_\xi\omega_\eta\right)\frac{\partial r}{\partial t}-\frac{1}{J}\left(r_\eta\omega_\xi-r_\xi\omega_\eta\right)\frac{\partial z}{\partial t}+\frac{1}{r}\frac{1}{J^2}\left(-r_\eta\psi_\xi+r_\xi\psi_\eta\right)\left(z_\eta\omega_\xi-z_\xi\omega_\eta\right)$$
$$-\frac{1}{r}\frac{1}{J^2}\left(z_\eta\psi_\xi-z_\xi\psi_\eta\right)\left(-r_\eta\omega_\xi+r_\xi\omega_\eta\right)-\frac{1}{r^2}\frac{1}{J}\omega\left(-r_\eta\psi_\xi+r_\xi\psi_\eta\right)$$
$$=\nu\frac{1}{J^2}\left(\alpha\omega_{\xi\xi}-2\beta\omega_{\xi\eta}+\gamma\omega_{\eta\eta}\right)+\nu\frac{1}{r}\frac{1}{J}\left(z_\eta\omega_\xi-z_\xi\omega_\eta\right)-\nu\frac{1}{r^2}\omega$$
$$+\frac{1}{J}Bg\left(z_\eta T_\xi-z_\xi T_\eta\right)+\frac{1}{J}Gg\left(z_\eta C_\xi-z_\xi C_\eta\right), \tag{23}$$

$$L_{SL}\rho\frac{\partial f}{\partial t}=-\kappa_L\frac{1}{r_\xi}\frac{1}{J_L}\left(-\beta T_\xi+\gamma T_\eta\right)_L+\kappa_S\frac{1}{r_\xi}\frac{1}{J_S}\left(-\beta T_\xi+\gamma T_\eta\right)_S, \text{ and} \tag{24}$$

$$\left(C_L-C_S\right)\frac{\partial f}{\partial t}=-D_L\frac{1}{r_\xi}\frac{1}{J_L}\left(-\beta C_{L\xi}+\gamma C_{L\eta}\right)_L, \tag{25}$$

where, $\alpha=r_\eta^2+z_\eta^2$, $\beta=r_\xi r_\eta+z_\xi z_\eta$, $\gamma=r_\xi^2+z_\xi^2$, $J=r_\xi z_\eta-r_\eta z_\xi$, $\xi$, and $\eta$ are the computational coordinates corresponding to $r$ and $z$ in the physical space, $\psi$ the stream function, $\omega$ vorticity, $T$ temperature, $\rho$ density, $C_p$ specific heat, $\kappa$ thermal conductivity, $\nu$ kinetic viscosity, $L_{SL}$ latent heat, $B$ thermal volume expansion coefficient, $G$ the buoyancy coefficient by the specific gravity difference, $g$ gravity, $t$ time, $C$ the concentration, $D$ the diffusion coefficient. Subscripts of $L$ and $S$ indicate the liquid side and the solid side, respectively. By numerically solving the simultaneous equations, Eqs. (19)-(25), the two-dimensionality is calculated. The typical result of concentration distribution in a grown crystal under no gravity condition is shown in Fig. 4. In this simulation, a seed crystal made of InGaAs and a crucible made of BN is assumed. The sample diameter is 20 mm. This is a target diameter in the microgravity experiment. This figure shows that the interface is strongly curved and is concave towards melt. In addition, the radial uniformity of the concentration seems to be not good. In this case, it is expected that the two-dimensionality is also not good.

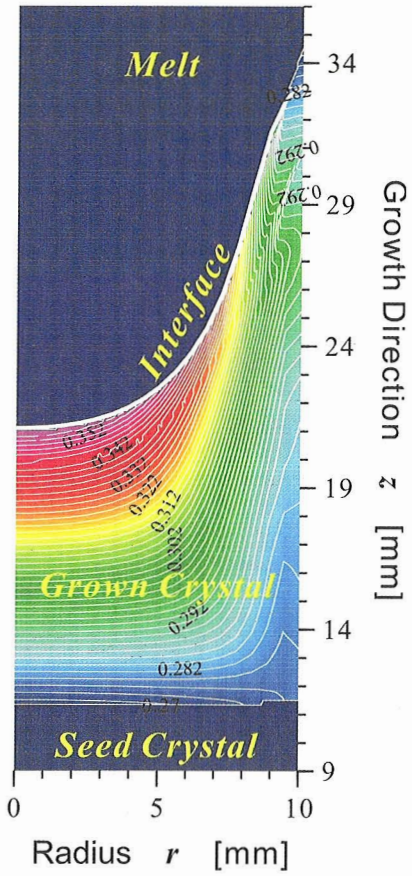


**Fig. 4** Concentration distribution in grown crystal under no gravity condition

## 4. Results and Discussion

The typical results of the radial two-dimensionality distributions in a combination of a InGaAs sample and a BN crucible under the 1 $g$ and $10^{-5}$ $g$ conditions are shown in Fig. 5. From Fig. 4, it is found that the two-dimensionality under the microgravity condition is smaller than that under 1 $g$ condition at almost all radii except for radii near the wall. The microgravity should cause this two-dimensionality improvement due to the convection suppression. However, the microgravity is not effective for the two-dimensionality reduction near the wall. This is reasonable since the convection is weak near the wall even in 1 $g$ due to the wall effect. In addition, these results indicate that another mechanism increasing the two-dimensionality near the wall should exist. Here, we focus on thermal conductivity differences. The thermal conductivity of the InGaAs seed crystal and the BN crucible are 3.0 W/m K and 23.7 W/m K, respectively. The conductivity of the crucible is about eight times larger than that of the seed crystal. This difference of the thermal conductivity should affect the heat flux between melt and the crucible and that between the crucible and the seed crystal. If this hypothesis, that is, the increase of the two-dimensionality near the wall is caused by the thermal conduction, is correct, another combination of the seed crystal and the crucible materials will be improve the two-dimensionality.

In order to confirm this hypothesis, large thermal conductivity of the seed crystal is used in the simulation, that is, 16 W/m K, which is the thermal conductivity of GaAs. The concentration distribution of the grown crystal is shown in Fig. 6. By comparing the contours in Fig. 6 with that in Fig. 4, it is clearly observed that the radial concentration gradient in Fig. 6 is much smaller than that in Fig. 4. This is caused by only the increase of the thermal conductivity of the seed crystal. In the

GaAs seed case, the two-dimensionality is also improved to about 25 % of that in the InGaAs seed case as shown in Fig. 7. However, the two-dimensionality in the GaAs seed case is still about 20 %. This may cause the gentle homogeneity deterioration. In order to improve the two-dimensionality further more, the thermal conductivity of the crucible is set to 5 W/m K. This corresponds to fused quartz. Figure 8 shows the summary of these two-dimensionality calculations. In this figure, the radial profiles of the concentration is plotted. From this figure, it is found that the homogeneity in the 5.0 W/m K case is the most excellent. The homogeneity may not be measured experimentally in this case.

In order to clarify the influence of the crucible material on the two-dimensionality, the thermal conductivity of the crucible widely varies in the simulation. The result is summarized and is shown in Fig. 9. From this figure, it is found that the two-dimensionality in the 5 W/m K case is much smaller than that in the 23.7 W/m K case. Thus the combination of the GaAs seed crystal and the fused quartz crucible is the best to obtain the homogeneous crystal. These results indicate that the hypothesis that the thermal conduction dominates the two-dimensionality near the wall should be correct.

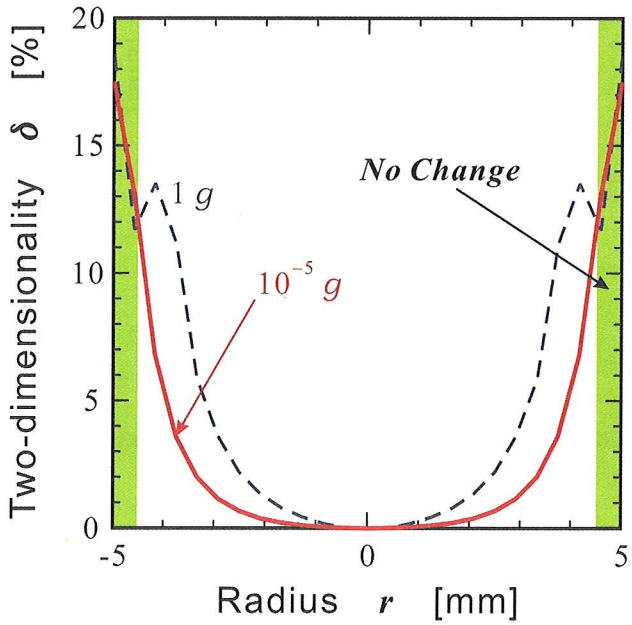


**Fig. 5** Typical results of radial two-dimensionality distributions

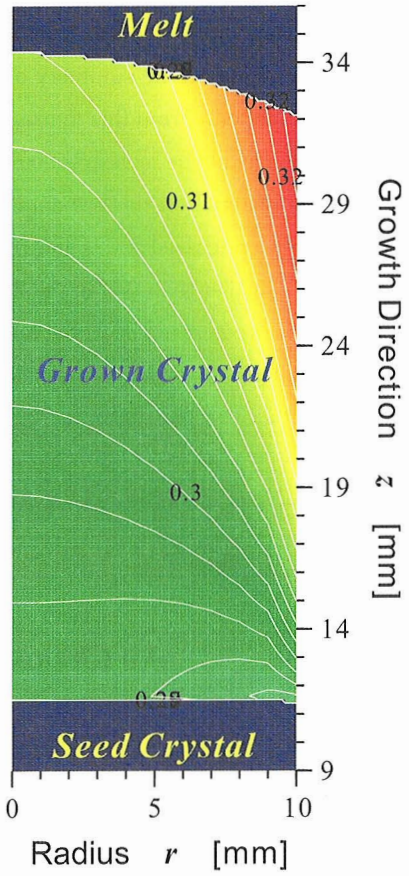


**Fig. 6** Concentration distribution in grown crystal under no gravity condition

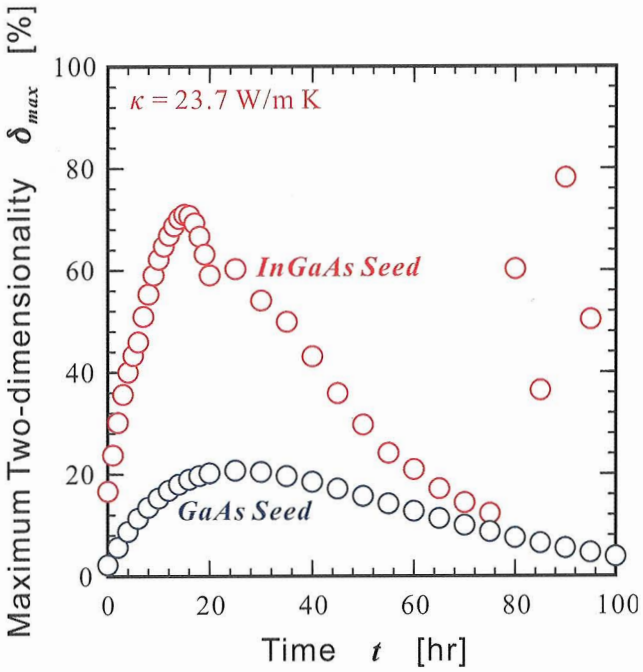


**Fig. 7** Time evolution of the maximum two-dimensionality

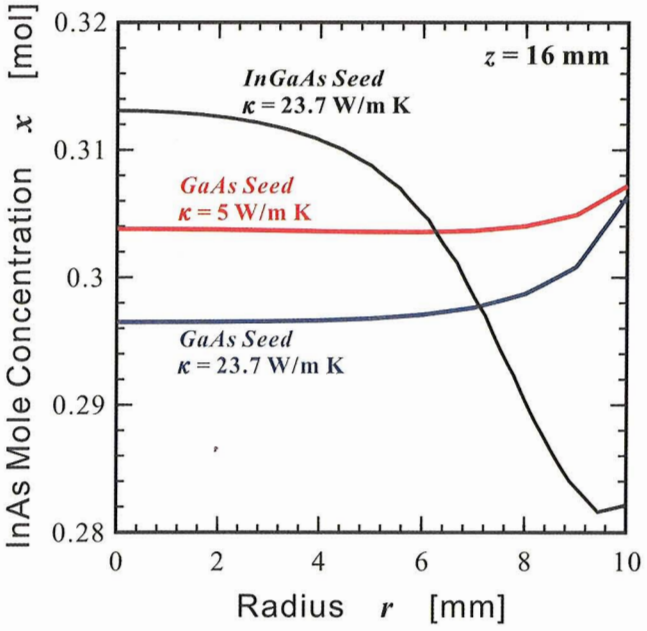


Fig. 8 Radial concentration profiles in grown crystals

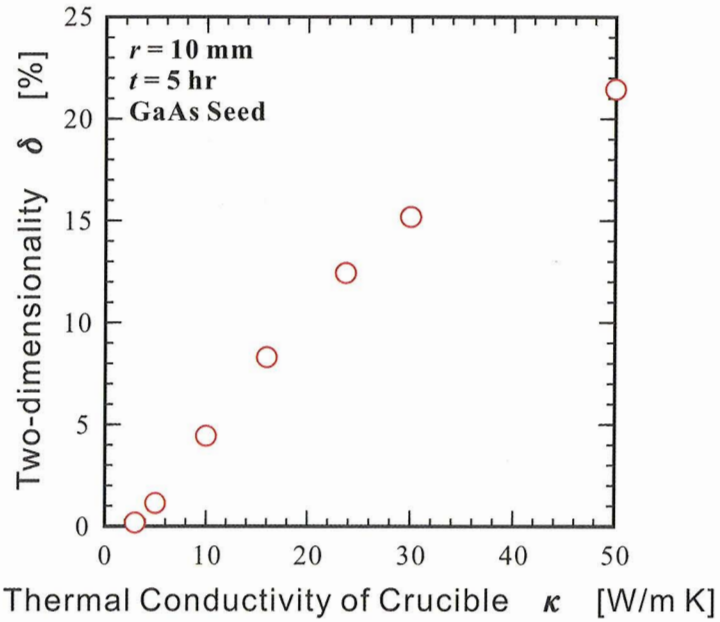


Fig. 9 Dependency of Two-dimensionality on thermal conductivity of crucible

## 5. Conclusions

The convection influence index $\chi$ is not zero when the convection is sufficiently suppressed. We consider this phenomenon is caused by the thermal conduction influence. Thus a new index named the two-dimensionality is introduced through the theoretical modeling of the TLZ method. To calculate the two-dimensionality, numerical simulation is carried out. In a case of a sample diameter of 20 mm, it is found that a combination of an InGaAs seed crystal and a BN crucible is inappropriate from the viewpoint of homogeneity. Therefore, more appropriate combination of a seed and a crucible materials is investigated. First, the combination of GaAs seed crystal and the BN crucible is tried.

Although this combination drastically decrease the two-dimensionality, it may not be sufficiently small. Then we use the combination of GaAs seed crystal and the fused quartz crucible. From the simulation, it is found that this is the best combination from the viewpoint of the homogeneous crystal growth. By using this combination, a homogeneous crystal with 20 mm in diameter will be obtained in microgravity experiments. In addition, these results indicate that the thermal conduction dominates the two-dimensionality near the wall. However, the GaAs seed crystal may cause polycrystallization. Therefore, a doped InGaAs crystal, of which thermal conductivity is similar to the GaAs crystal, will be required. In addition, the fused quartz crucible may disturb single crystal growth. These potential problems will be solved in future works.

## References


[1] K. Kinoshita, H. Kato, M. Iwai, T. Tsuru, Y. Muramatsu, S. Yoda, "Homogeneous In0.3Ga0.7As crystal growth by the traveling liquidus zone method", J. Cryst. Growth, **225**, 59-66 (2001).

[2] K. Kinoshita, Y. Hanaue, H. Nakamura, S. Yoda, M. Iwai, T. Tsuru, Y. Muramatsu, "Growth of homogeneous mixed crystals of $In_{0.3}Ga_{0.7}As$ by the traveling liquidus-zone method", J. Cryst. Growth, **237-239**, 1859-1863 (2002).

[3] H. Nakamura, Y. Hanaue, H. Kato, K. Kinoshita and S. Yoda, "A one-dimensional model to predict the growth conditions of $In_xGa_{1-x}As$ alloy crystals grown by the traveling liquidus-zone method", J. Cryst. Growth, **258**, 49-57 (2003).

[4] S. Adachi, Y. Ogata, N. Koshikawa, S. Matsumoto, K. Kinoshita, M. Takayanagi and S. Yoda, "Convection influence on mass transport in the traveling liquidus-zone method", J. Cryst. Growth, **267**, 417-423 (2004).

[5] J. F. Thompson, F. C. Thames and C. W. Mastin, "Automatic numerical generation of body-fitted curvilinear coordinate system for field containing any number of arbitrary two-dimensional bodies", J. Comp. Phys., **15**, 299-319 (1974).

[6] K. Fujii, "Numerical Methods for Computational Fluid Dynamics", Tokyo Univ., Tokyo, Chap. 7 (1994) [in Japanese].

[7] H. Takami and T. Kawamura, "Numerical Solution of Partial Differential Equations by the Finite Difference Method", Tokyo Univ., Tokyo, Chap. 6 (1994 ) [in Japanese].

[8] J. S. Szmyd and K. Suzuki (Ed.), "Modeling of Transport Phenomena in Crystal Growth", WIT Press, Southampton, Chap. 4, (2000).

[9] S. Adachi, K. Kawachi, M. Kaneko, H. Kato, S. Yoda and K. Kinoshita, "Reliability Investigation on Numerical Analysis by Comparison with Experimental Result", Annual Report of the Semiconductor Team in NASDA Space Utilization Research Program, (2000).

[10] S. Adachi, S. Yoda, and K. Kinoshita, "Numerical Analysis of a Cartridge in the Traveling Liquidus-Zone Method under Various Gravity Conditions", Annual Report of the Semiconductor Team in NASDA Space Utilization Research Program, (2001).

[11] S. Adachi, N. Koshikawa, S. Matsumoto, S. Yoda, and K. Kinoshita, "Numerical Investigation on Two-dimensionality in a Flight Cartridge", Annual Report of the Semiconductor Team in NASDA Space Utilization Research Program, (2003).